

Research Article

Steady Air Injection Flow Control Parameters in a Transonic Axial Compressor

Islem Benhegouga and Yang Ce

Department of Mechanical Engineering, Beijing Institute of Technology, Beijing, 100081, China

Abstract: In the present study, steady air injection upstream of the tip blade leading edge was studied. To reveal the mechanism, steady numerical simulations were performed on a transonic axial compressor, NASA rotor 37. The injection angle α is 20° and three injector axial position were studied, respectively 9, 18 and 27% upstream of the axial chord length at blade tip (ca). For each position a different injection mass flow rate and different injection yaw angles were simulated. The results show at design speed ($n = 17188$ r/min), with injector position at 9% ca, injection mass flow rate of 2% and injection yaw angle between -20° and -30° , the mass flow rate at stall can decrease for approximately 3%, but others compressor parameters were affected such as the total pressure ratio. With injector positioned at 27% ca, the decrease in the mass flow rate at stall is less obvious, but the effect on the compressor pressure ratio is benefic.

Keywords: Air injection, numerical simulation, transonic axial compressor

INTRODUCTION

All current research on compressors, focus exclusively on the best way to eliminate instabilities, such as surge or stall, which affect the efficient functioning of the system and cause various losses in yield and rate of pressure. Recent research results (Lin *et al.*, 2008; Vo *et al.*, 2008) suggested the Tip Leakage Flow (TLF) and its interaction with the incoming main flow to be responsible for spike-type stall precursor and rotating stall inception. The pressure difference across the blade causes a leakage flow through the tip clearance from the pressure surface to the suction surface of the blade.

Flow through the tip gap interacts with the incoming passage flow near the suction side of the blade as it leaves the blade tip section, forming the tip clearance vortex. The vortex core is formed by fluid originating from the leading edge of the blade. Fluid flowing over the remainder of the blade rolls around this core vortex and adds swirl intensity. Some tip clearance flow originating near the casing travels over to the tip gap of the adjacent blade, resulting in so-called double leakage flow (Smith, 1993).

Near the stall condition, the pressure difference across the blade tip section increases and the interaction between the tip clearance flow and the passage flow becomes stronger. This causes more mixing losses and an increase in aerodynamic blockage near the casing.

To minimize the adverse effects of tip clearance flow field in compressors, many flow control strategies was studied. Casing treatments (Müller *et al.*, 2007;

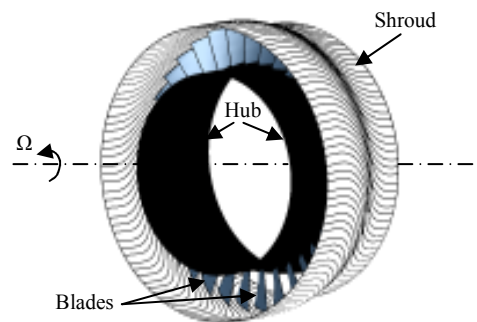


Fig. 1: NASA rotor 37

Aamir and John, 2005; Wilke and Kau, 2002), air injection (Behnam *et al.*, 2006; Khaleghi *et al.*, 2004; Chunhua and Michael, 2004; Jinwoo *et al.*, 2003; Suder *et al.*, 2001), plasma actuation (Robert *et al.*, 2011), inlet recirculation (Masahiro *et al.*, 2006, 2004), are representative examples of tip clearance flow control.

In this study we will try to see the effects of an active control that is control by steady flow injection at the casing wall of a transonic axial flow compressor which is the experimental NASA Rotor 37 (Rodrick, 2009; Lonnie and Royce, 1978). The approach used and results obtained will be discuss in the rest of this study.

COMPRESSOR USED AND NUMERICAL METHOD

The experimental compressor NASA rotor 37 (Fig. 1) is used for the investigation presented. The

Corresponding Author: Islem Benhegouga, Department of Mechanical Engineering, Beijing Institute of Technology, Beijing 100081, China

This work is licensed under a Creative Commons Attribution 4.0 International License (URL: <http://creativecommons.org/licenses/by/4.0/>).

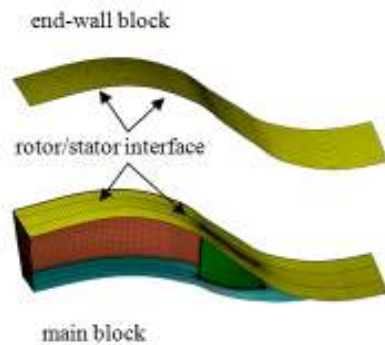


Fig. 2: Computational grid

NASA rotor 37 has 36 rotor blades, at design point it operates at speed of 17188 rpm and has a total pressure ratio of about 2.1. The relative Mach number at blade tip is about 1.5 and the design tip clearance is estimated to be 0.356 mm which is about 0.5% span.

The numerical solver NUMECA/ERANUS was used for the simulation. The rotor computational grid was generated in IGG/AUTO-GRID; structured H-type grids were generated for the inlet and the outlet and a main O-block surrounding the rotor blade. The generated mesh is divided into two parts. The first one or the main block includes the whole blade and 50% of the tip gap which is about 0.178 mm. the second part includes the rest of tip gap. Figure 2 shows the computational grid, both grids have 193 stream-wise nodes and 41 nodes in the blade-to-blade direction and for the span-wise direction the main block consists of 41 nodes and the secondary block consists of 9 nodes. The overall mesh size used in the computation is 797256 cells, 677340 cells for the main block and 119916 for the end-wall block.

The purpose of this division is to create a sliding interface, because when we add the injector block we can't do a real connection with the main block of the

compressor, because the faces are not the same, one is static (injector face) and the second one is a rotating surface (rotor block), so we have to introduce a teeny block upstream the main block of the compressor and which is a static block. In this way we can connect the main block with the end-wall block by using a ROTOR/STATOR connection and the injector block with the whole block by using FNMB connection.

The whole mesh quality is as follow, the orthogonality of all grids was larger than 10° and aspect ratio was less than 500 and expansion ratio were less than 3. And the first grid spacing ensure $y^+ < 10$ at the walls which makes the boundary layer simulation reliable.

The numerical simulations were performed by solving the steady compressible Navier-Stokes equation using the FINE/TURBO software package. The 3D Reynolds-averaged N-S equations were discretized in space using a cell-centered finite volume method with a second-order centered difference scheme and in time using a 4-stage Runge-kutta integration method. As for turbulence model, the Spalart-Allmaras one formulation turbulence model was employed. Additionally, a full multilevel grid method and implicit residual smoothing method were used for speed up the convergence of calculation. For boundary conditions, at the inlet total pressure, total temperature and flow angle distribution were specified. A constant static pressure was prescribed at the exit to adjust the mass flow rate. Different working point on a constant speed line can reach by increasing the exit static pressure.

Figure 3 shows a schematic of the injector system, the injectors are positioned over the blade tip region at different distances, $d = 9, 18$ and 27% of the tip chord upstream of the blade leading edge, the injection angle is " $\alpha = 20^\circ$ " and the yaw angle " β " is a parametrically variable, negative yaw angle were measured relative to the compressor face in opposite direction of rotational speeds.

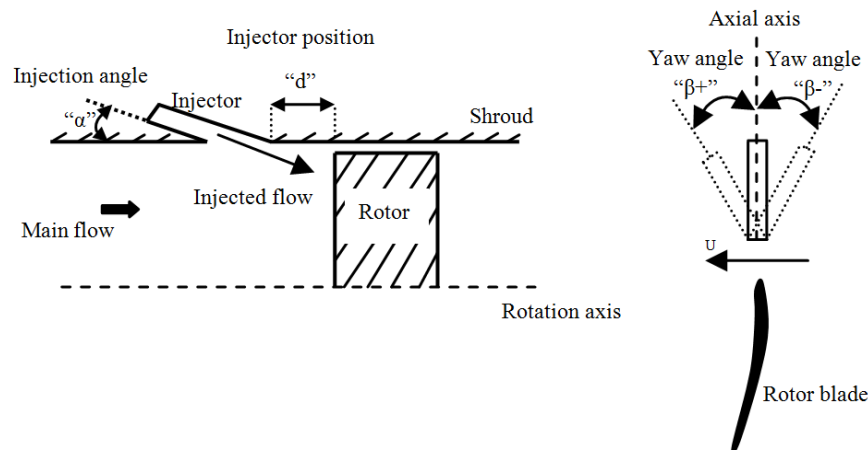


Fig. 3: Schematic of the injection and injector geometry

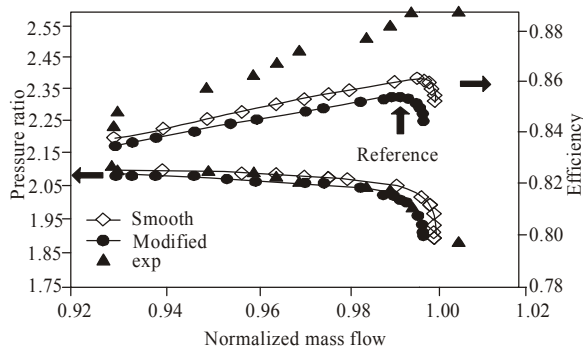


Fig. 4: Computed and measured NASA rotor 37 characteristics profile

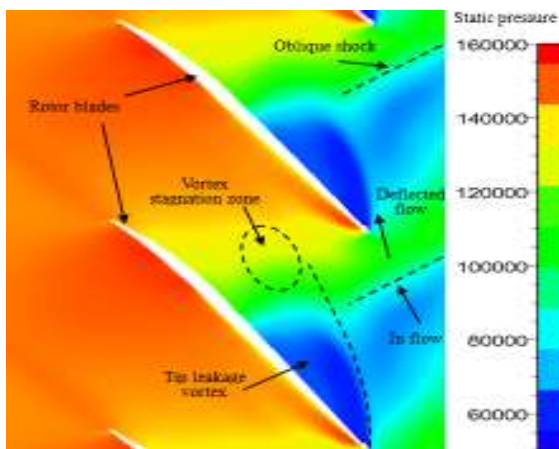


Fig. 5: Static pressure distribution near stall region and at design speed for the NASA rotor 37

Validation of the simulation model: Figure 4 compares the computed and experimental measured compressor maps at design speed. The experimental data for the NASA rotor 37 in the current work have been published in a report by the ASME (1994) turbo-machinery committee. The numerical results are for the NASA rotor 37 with and without the static end wall block. The numerical simulation reveal at design speed a maximum mass flow of 20.82 Kg/s this is inside the tolerance of experimental value (20.93±0.14 Kg/s). The computed pressure ratio for the compressor without end wall block agree very well with the experiment, however the maximum efficiency obtained is less about 2% than that obtained from the experiment. The results obtained from the simulation of the rotor 37 with the end wall block are not as good as those obtained without the end wall modification. These differences have been observed by other authors who numerically investigated the NASA rotor 37, NASA investigations revealed that this is due to the presence of high axial gap in hub annulus line upstream of the blade leading edge, which has detrimental effects on the compressor proprieties (Dunham, 1998). Therefore, it can be concluded that the numerical model used is able to reveal all important flow mechanisms, which are

essential for understanding the influence of the steady tip flow injection control.

Flow behavior and characteristics in the NASA rotor 37: Figure 5 shows the distribution of static pressure at 95% of span, at 100% design speed and close to stall region. We can see how the main flow is deviated because of the blockage due to the large stagnation zone.

The explanation of this phenomenon is that near the blade tip the inflow angle of attack is very high, so the main flow cannot follow the direction which is given by the blade geometry, this will cause a flow separation on the suction side of the blade and a significant deceleration of the inflow at the upstream part of the suction side. Flow through the tip gap interacts with the separate flow from the blade suction side forming the tip clearance vortex. Fluid flowing over the remainder of the blade rolls around this core vortex and adds swirl intensity, this cause the formation of a stagnation zone that blocking the incoming main flow.

Figure 6 shows the distribution of the relative Mach number near the blade tip plotted on equally spaced cutting planes, at 100% design speed and for two different cases of compressor characteristics, one is the case of the maximum efficiency and the second one is the case near stall region. The black streamlines represent the main flow and the red ones represent the tip leakage vortex.

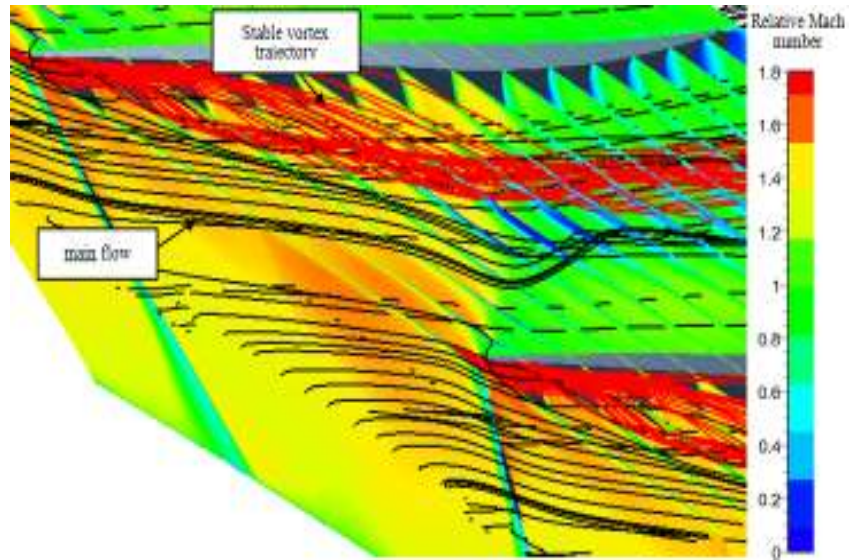
At maximum efficiency, the stagnation vortex zone is very small and don't affect the main flow passage. The stagnation zone is larger in the second case (near stall region) and blocks the main flow near the leading edge and cause a deflection in the inflow against the blade rotation.

Effect of tip injection: It is well known that the end-wall fluid near the blade tip is an unstable low-momentum fluid and this causes the back flow and can lead to stall. So by injecting fluid in this region, we can energize the retarded flow as shown in Fig. 7.

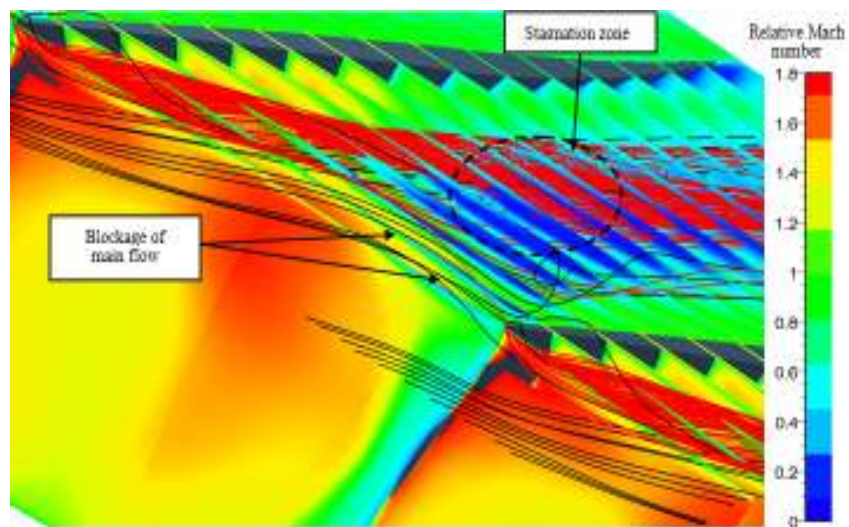
In this study, to illustrate the effects of such control and to better understanding of his effectiveness in axial transonic turbo-compressor, we will introduce the relationship of stall margin, denoted as NASA standard stall margin, which is defined by Royce and Lonnie (1980) as:

$$SM = \left(\frac{\pi_{stall} \times \dot{m}_{ref}}{\pi_{ref} \times \dot{m}_{stall}} - 1 \right) \times 100$$

The choice of the reference point is an arbitrary choice, of such a kind that we can compare the results of this formula to a common point. We opted for the point of maximum efficiency as a reference point and this point corresponds to:



(a)



(b)

Fig. 6: Relative mach number distribution for the NASA rotor 27, (a) maximum efficiency, (b) near stall region

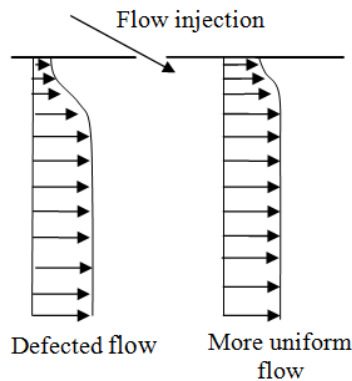


Fig. 7: Illustration of flow injection effect on the end-wall flow

$$\dot{m}_{ref} = \dot{m}_{\eta_{max}} = 99.375\% \text{ of } \dot{m}_{choke}$$

$$\pi_{ref} = \pi_{\eta_{max}} = 2.029$$

In this study three axial positions of the injectors were studied, respectively 9, 18 and 27% upstream of the axial chord length at blade tip. Figure 8 shows the stall margin plotted as bar charts for the second axial position of the injectors (18% upstream of the axial chord length at blade tip), three different injection mass flow rates ($\dot{m}_{ing1} = 1.5\%$, $\dot{m}_{ing2} = 2\%$ and $\dot{m}_{ing3} = 2.5\%$) have been considered and for each injection mass flow rate various injection yaw angles ($+20^\circ$, 0° , -20° , -30° and -40°) have been simulated. We can see an

improvement in stall margin of over 2.4% for an injection mass flow rate between 1.5 and 2% and for yaw angle between -20° and -30° , we also not that the positive yaw angle affect negatively the stall margin.

Figure 9 shows the stall margin plotted as bar charts for the first axial position of the injectors (9% upstream of the axial chord length at blade tip), four different injection mass flow rates ($\dot{m}_{inj1} = 1.25\%$, $\dot{m}_{inj2} = 1.5\%$, $\dot{m}_{inj3} = 1.75\%$ and $\dot{m}_{inj4} = 2\%$) have been considered and

for each injection mass flow rate various injection yaw angles (-20° , -30° and -40°) have been simulated, we can see that more the injection mass flow rate is high more the stall margin is big and he can reach 2.92%, but the best yaw angel steel between -20° and -30° .

In Fig. 10 only one injection mass rate $\dot{m}_{inj} = 3\%$ and three yaw angles (-20° , 30° and -40°) have been presented, the injectors were positioned at 27%

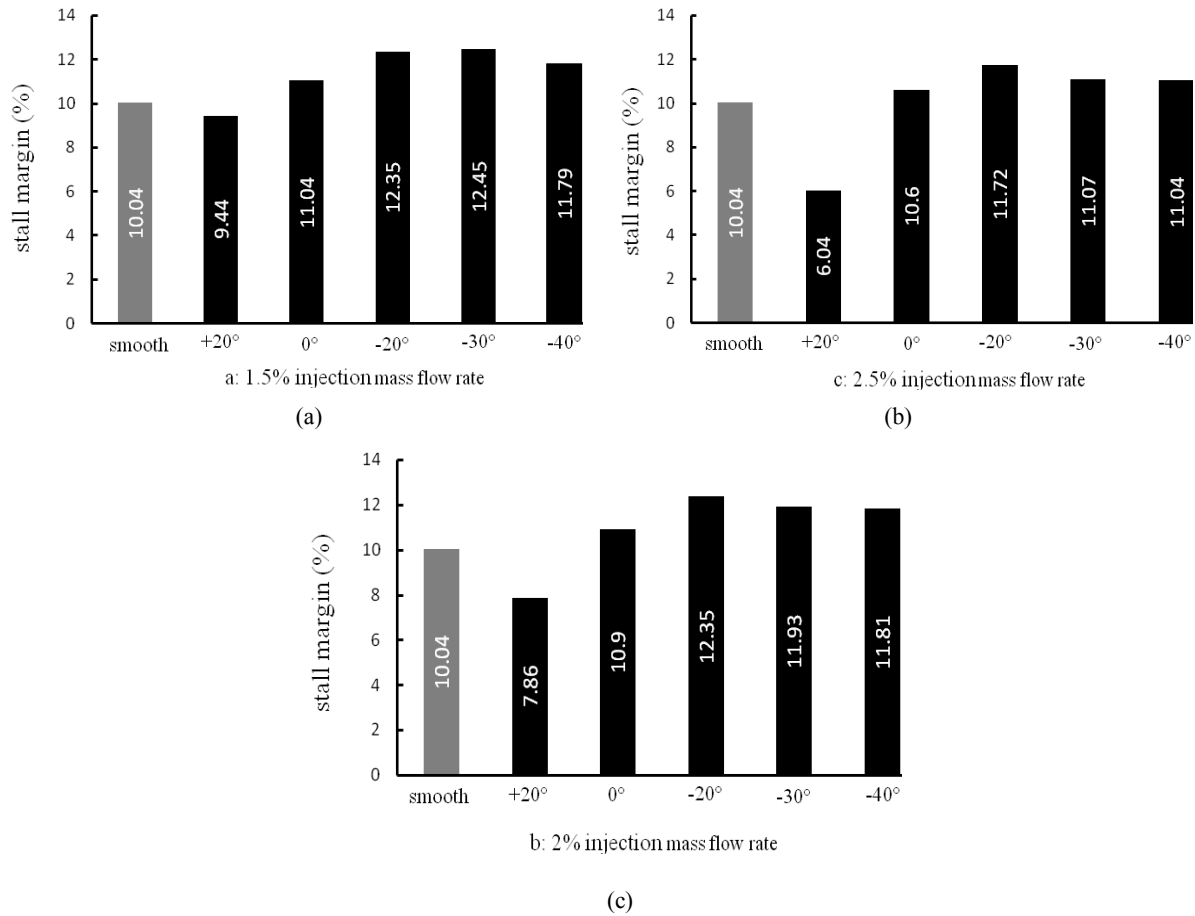
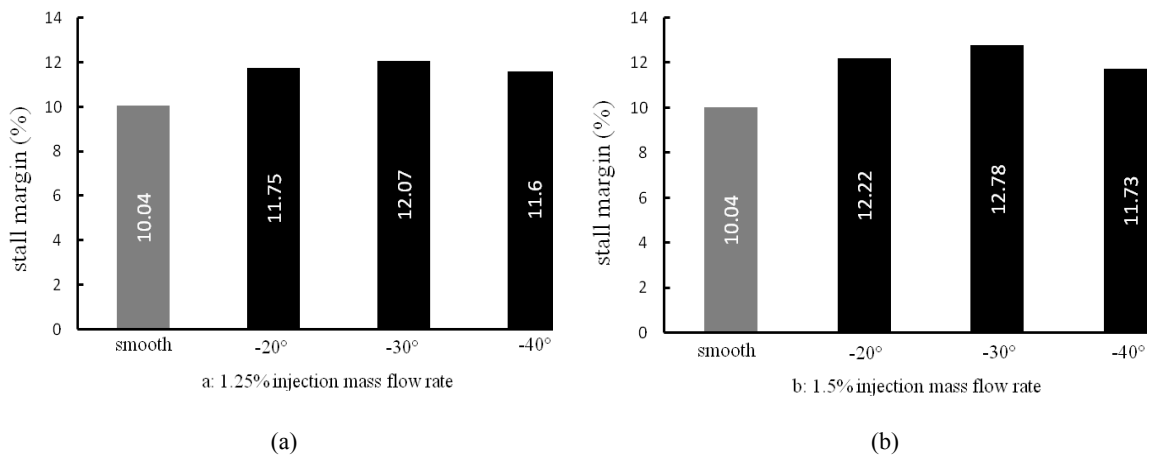


Fig. 8: Effect of tip injection on stall margin for an axial position of the injector of 18% upstream of the blade chord length at blade tip



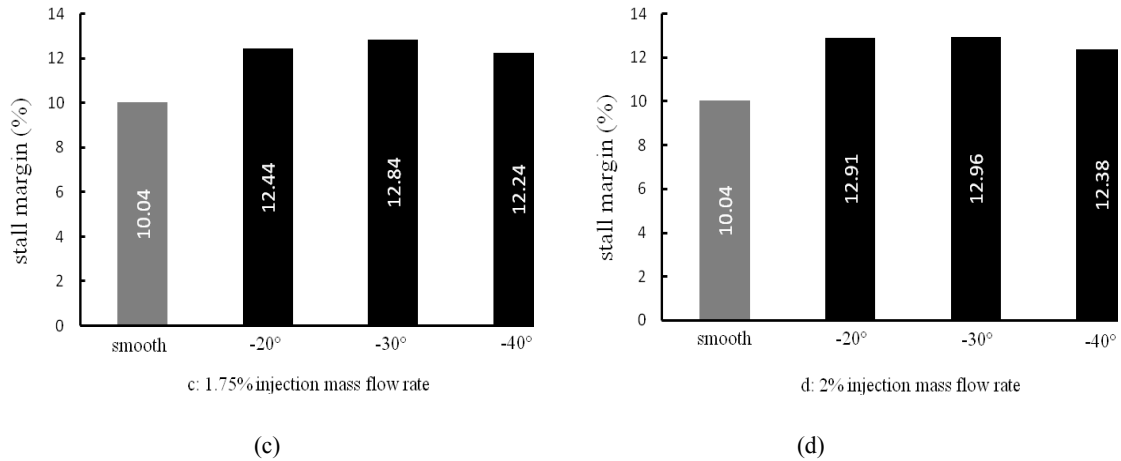


Fig. 9: Effect of tip injection on stall margin for an axial position of the injector of 9% upstream of the blade chord length at blade tip

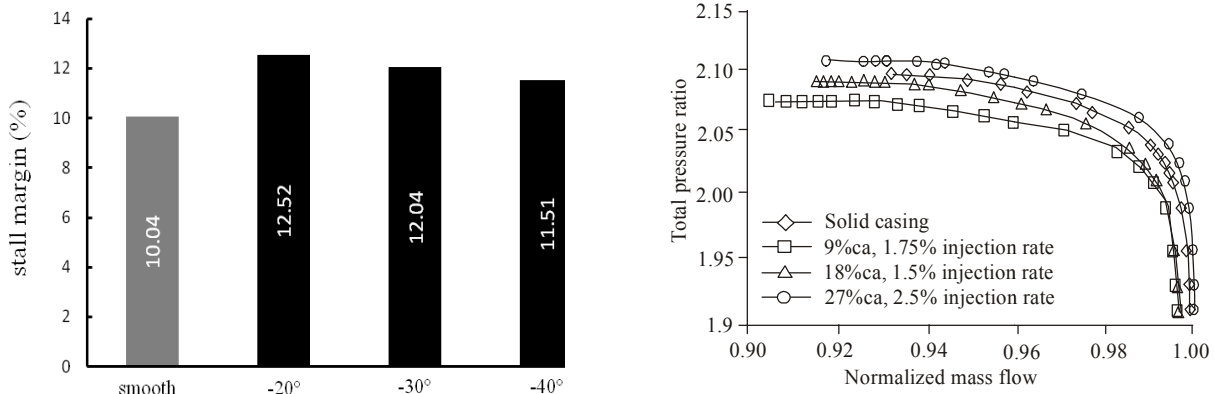


Fig. 10: Effect of tip injection on stall margin for an axial position of the injector of 27% upstream of the blade chord length at blade tip

upstream of the axial chord length at blade tip. We can see an improvement in stall margin of over 2.5% at -20° yaw angle.

Before we get a conclusion about the best schema of this control, we have to see the effect of each axial position of the injectors on the compressor characteristics (total pressure ratio and efficiency). The overall effects of tip injection on the compressor total pressure ratio and efficiency are presented in Fig. 11.

The results shown in this figure are for a yaw injection angle equal to -20° and the injection rate used for each injector axial position is the one which gives the best stall margin. (ca) in the figure legend means the axial chord length at blade tip. The mass flow is normalized by the inlet mass flow rate. We can observe that the more the injector is close to the blade leading edge the more the mass flow rate at stall is decreased but also the losses on the compressor characteristics are more significant, the loss in efficiency can reach 0.12% and

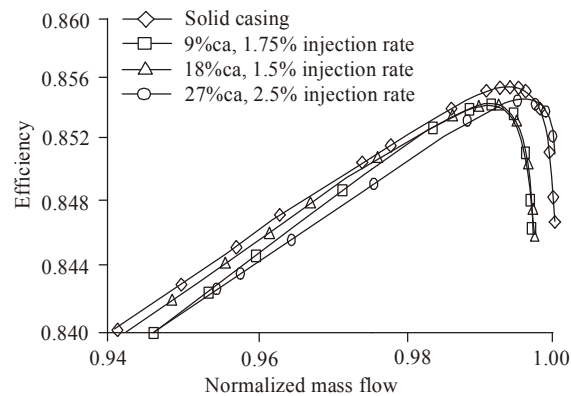


Fig. 11: Effect of tip injection on compressor pressure ratio and efficiency

the loss in the total pressure ratio can reach 1%. In the other hand, the more the injector is far from the blade leading edge the more the decrease in the stall mass flow is small, but we can get a beneficial effect on the compressor total ratio which can reach 0.5% and a very small degradation on the compressor efficiency.

We will also use the formula defined by Hathaway (2002), which helps as to calculate the stable range

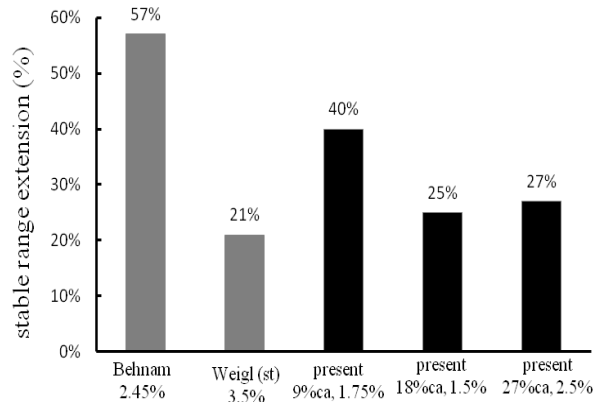


Fig. 12: Comparison of the stable range extension between the current design and others tip injection design

extension of our schema of control and we will use this results to compare them with those calculated from other schemas of the same control type (Khaleghi *et al.*, 2004; Weigl *et al.*, 1998).

$$SRE = \frac{(\dot{m}_{choke} - \dot{m}_{stall})_{injection} - (\dot{m}_{choke} - \dot{m}_{stall})_{smooth}}{(\dot{m}_{choke} - \dot{m}_{stall})_{smooth}} \times 100$$

The results are plotted in the Fig. 12. The range extension predicted by the present study can reaches 40% for injector axial position equal to 9% ca, injection yaw angle equal to -20° and injection mass flow rate of 1.75%. We can observe that the more the injector is close to the blade leading edge the more the stability is significant.

CONCLUSION

In this study, a tip injection flow control in a transonic axial compressor, NASA rotor 37, is studied by using numerical simulation. For the effectiveness of this control some parameters must be carefully chosen, such as the injector axial position, injection yaw angle and the injection mass flow rate. From the compression system studied in this study, we can get:

- The axial position of the injectors is very important for the enhancement of the compressor stall margin and the compressor total pressure ratio. For a high stall margin, the injector must be close to the tip blade leading edge and for a better total pressure ratio of the compressor, it must be a little far from the tip blade leading edge.
- Yaw angle setting between -20° and -30° yielded best injection results.
- The more the injection mass flow rate is high the more the stall margin is high and the more is the degradation in the compressor characteristics is important.

- The current control design shows an acceptable level of the compressor stability compared to others designs for injection flow control.

REFERENCES

- Aamir, S. and J.A. John, 2005. Flow mechanism for stall margin improvement due to circumferential casing grooves on axial compressors. ASME J. Turbomach., (127): 708-717.
- ASME Turbomachinery Committee, 1994. CFD Code Assessment in Turbomachinery - Data Report, Distribution to the Participant of the Code Assessment Exercise.
- Behnam, H.B., G. Kaveh, F. Bijan, A.T. Joao and C.I. Paul, 2006. A new design for tip injection in transonic axial compressors. ASME Turbo Expo. Barcelona, Spain, ASME: GT2006-90007, pp: 39-47.
- Chunhua, S. and R. Michael, 2004. Numerical simulations of rotor 35 with and without tip injection using an arbitrary mach number flow solver. 42nd AIAA aerospace sciences meeting and exhibit, Reno, Nevada.
- Dunham, J., 1998. CFD Validation for propulsion system components. AGARD Advisory Report 355, ISBN: 92- 836-1075-X.
- Hathaway, M.D., 2002. Self-Recirculating Casing Treatment Concept for Enhanced Compressor Performance. ASME Turbo Expo. Amsterdam, The Netherlands, ASME: GT-2002-30368, pp: 411-420.
- Jinwoo, B., S.B. Kenneth and S.T. Choon, 2003. Active control of tip clearance flow in axial compressors. ASME turbo expo. Atlanta, Georgia, USA, ASME: GT2003-38661.
- Khaleghi, H., J.A. Teixeira, A.M. Tousei and M. Boroomand, 2004. Parametric study of injection angle effects on stability of transonic axial compressors. Propul. Pow. J., 24(5): 1100-1107.
- Lin, F., J.X. Zhang, J.Y. Chen and C.Q. Nie, 2008. Flow structure of short length scale disturbance in an axial flow compressor. AIAA J. Propul. Pow., 24(6): 1301-1308.
- Lonnie, R. and D.M. Royce, 1978. Design and Overall Performance of Four Highly Loaded high Speed Inlet Stages for an Advanced high Pressure Ratio Core Compressor. National Aeronautics and Space Administration, Washington, pp: 119.
- Masahiro, I., S. Taufan, U. Hironobu and S. Daisaku, 2004. Suppression of unstable flow at small flow rates in a centrifugal blower by controlling tip leakage flow and reverse flow. ASME Turbo Expo. Vienna, Austria, ASME: GT2004-53400, pp: 761-770.
- Masahiro, I., D. Sakaguchi and H. Ueki, 2006. Effect of pre-whirl on unstable flow suppression in a centrifugal impeller with ring groove arrangement. ASME Turbo Expo. Barcelona, Spain, ASME: GT2006-90400, pp: 1049-1057.

- Müller, M.W., H.P. Schiffer and C. Hah, 2007. Effect of circumferential grooves on the aerodynamic performance of an axial single stage transonic compressor. ASME Turbo Expo. Montreal, Canada, ASME: GT2007-27365, pp: 115-124.
- Robert, C.M., E. Katherine, A.B. Grover and S. Seyed, 2011. Control of tip-clearance flow in a low Speed axial compressor rotor with plasma actuation. ASME J. Turbomach., (134): 1-9.
- Rodrick, V.C., 2009. Swift code assessment for two similar transonic compressors. NASA/TM, 2009-215520.
- Royce, D.M. and R. Lonnie, 1980. Performance of Single-Stage Axial-Flow Transonic Compressor with Rotor and Stator Aspect Ratios of 1.19 and 1.26, Respectively and with Design Pressure Ratio of 2.05. National Aeronautics and Space Administration, Washington, DC, pp: 103.
- Smith, L.H., 1993. Private communication.
- Suder, K.L., M.D. Hathaway, A.T. Scott, J.S. Anthony and B.B. Michelle, 2001. Compressor stability enhancement using discrete tip injection. ASME J. Turbomach., (123): 14-23.
- Vo, H.D., C.S. Tan and E.M. Greitzer, 2008. Criteria for spike initiated stall. ASME J. Turbomach., 130(1): 11-23.
- Weigl, H.J., J.D. Paduano, J.D. Frechette, A.H. Epstein, E.M. Greitzer, M.M. Bright and A.J. Strazisar, 1998. Active stabilization of rotating stall and surge in a transonic single-stage axial compressor. ASME J. Turbomach., 120: 625-636.
- Wilke, I. and H.P. Kau, 2002. A numerical investigation of the influence of casing treatments on the tip leakage flow in a hpc front stage. ASME Turbo Expo. Amsterdam, the Netherlands, ASME: GT2002-30642, 1155-1165.